ISSN 1060-992X, Optical Memory and Neural Networks (Information Optics), 2015, Vol. 24, No. 1, pp. 60–65. © Allerton Press, Inc., 2015.

Influence of the Metallic Nanoparticles on the Arabinogalactan Optical Properties

N. A. Ushakov, N. B. Radchuk, and A. Yu. Ushakov

St. Petersburg State Polytechnical University, St. Petersburg, Russia

e-mail: n.ushakoff@spbstu.ru

Received September 17, 2014; in final form, December 15, 2014

Abstract—Metallic nanoparticles are a powerful tool of modern photonics allowing one to modify and control the optical properties of materials. Arabinogalactan (AG)—a complex organic molecule, offers a convenient way for nanoparticle fabrication due to its chemical properties. In the current paper the refractive index and optical transparency of arabinogalactan and AG-nanoparticle composite was studied by means of wavelength-domain interferometry.

Keywords: metallic nanoparticles, wavelength-domain interferometry, arabinogalactan, refractive index measurement, dispersion measurement

DOI: 10.3103/S1060992X15010087

1. INTRODUCTION

Metallic particles with size about tens-hundreds nanometers attract the attention of a great number of researches during the last 10–15 years. In visible and infrared parts of optical spectrum their size become smaller than the wavelength of the optical radiation, thanks to that the properties of their interaction with light changes dramatically. One of the key phenomena, determining the optical properties of these nanoparticles, is collective oscillation of the conductivity electrons of the metal, i.e. excitation of plasmons [1, 2].

Such applications of metallic nanoparticles, as optical information processing, biophotonics, high-precision optical sensors, have been proposed and are under extensive development. The possibility of nanoparticles use in medical purposes, cosmetology is also under consideration [3, 4].

One of the problems, arising during the investigation and application of the metallic nanoparticles, is their capture and confinement in the analyte, keeping the required concentration. One of the solutions is the use of a composite material—a union of a nanoparticle with some relatively large molecule, acting as a nanoparticle carrier. Among the other materials, arabinogalactan (AG) is quite applicable for formation of such composites. Arabinoglactan [5, 6] is a complex organic material, consisting of arabinose and galactose monosaccharides. It is capable to capture the nanosized particles of metal during the chemical reduction of a salt, providing a convenient and easy way to produce such composites.

Wavelength-domain interferometry [7] (WDI) is a powerful tool, utilized in optical sensing of various physical quantities and also in measurement of various properties of transparent materials. In the WDI techniques the optical spectral function of the interferometer is registered, after that a special processing is performed on it in order to obtain the interferometer baseline value.

In the current paper an approach for refractive index and transmission measurement with the use of wavelength-domain interferometry is described and the results of application of the proposed approach to the AG metallic nanocomposites are presented. For that an extrinsic fiber Fabry–Perot interferometer was utilized.

2. WAVELENGTH-DOMAIN INTERROGATION OF FABRY–PEROT INTERFEROMETER

Strictly speaking, spectral transfer function $S(\lambda)$ of the Fabry–Perot interferometer is defined by the Airy function [8], for the reflected light from the interferometer it can be expressed as follows

$$S_{\mathrm{FP}}(L,\lambda) \cong \frac{R_1 + R_2^* + 2\sqrt{R_1 R_2^*}\cos\left(4\pi nL/\lambda + \gamma(L,\lambda)\right)}{1 + R_1 R_2^* + 2\sqrt{R_1 R_2^*}\cos\left(4\pi nL/\lambda + \gamma(L,\lambda)\right)}, \quad (1)$$

which, for the case of low finesse interferometer is simplified to a form

$$S_{FP}(L, \lambda) = S_0(L, \lambda) + S(L, \lambda), \tag{2}$$

$$S(L, \lambda) = S_M \cos(4\pi nL/\lambda + \gamma(L, \lambda)), \tag{3}$$

where $S_0(L, \lambda) = R_1 + R_2^*$, $S_M = 2(R_1 R_2^*)^{1/2}$; L is interferometer baseline; λ is the light wavelength; $\gamma(L, \lambda)$ is an additional phase shift caused by the mirrors and the beam diffraction (the so-called Gouy phase); n is refractive index of the media inside the interferometer, and in general case demonstrates wavelength dependence $n(\lambda)$; R_1 and R_2^* are the reflecting coefficients of the mirrors, the diffraction-induced light losses are included into the effective R_2^* value. For the practical case of Gaussian beam propagation [8] inside the cavity the effective reflection coefficient of the second mirror can be written as

$$R_2^*(L,\lambda) = R_2 \frac{\left(\pi n w_0^2\right)^2}{L^2\lambda^2 + \left(\pi n w_0^2\right)^2} \tag{4}$$

and the additional phase as [9]

$$\gamma(L,\lambda) = \operatorname{atan}\left[\frac{L\lambda}{\pi n w_0^2}\left(4\left(\frac{L\lambda}{\pi n w_0^2}\right)^2 + 3\right)\right] + \varphi, \tag{5}$$

where w_0 is an effective radius of a Gaussian beam at the output of the first fiber, close to the fiber mode field radius and φ is an additional phase shift, induced by the mirror (typically $\varphi = \pi$ for light reflected back to a less optically dense medium from a bound with a more optically dense medium).

After the interferometer spectral function $S'(\lambda)$ is measured, the interferometer baseline L can be found from it by various demodulation techniques. The simplest approach is based on the frequency estimation of a sinusoidal signal [10]. To do so, one needs to estimate the number of fringes N of the spectral function and then recalculate the baseline value according to the following expression [11]

$$L = \frac{N\lambda_{max}\lambda_{min}}{2\left(n_0 - \lambda_0 \frac{dn}{d\lambda}\right)(\lambda_{max} - \lambda_{min})}, \tag{6}$$

where λ_{min} and λ_{max} are the boundary wavelengths of the spectra measurements, λ_0 is the mean wavelength, n_0 is the mean value of the refractive index on the spectral interval of analysis.

One of the most attractive approaches for estimation of the baseline L from the registered spectrum $S'(\lambda)$ is to approximate it with known analytical expression describing the interferometer transfer function $S(\lambda, L)$ by means of least-squares fitting [12, 13]. Such fitting returns the global minimum of the residual norm, which is given by the expression

$$R(L) = \left\| S'(\lambda) - S(L,\lambda) \right\| = \sqrt{\sum_i \left[S_i' - S_i(L) \right]^2}, \tag{7}$$

where $S_i' = S'(\lambda_i)$, $S_i(L) = S(\lambda_i, L)$, $\lambda_i = \lambda_0 + i\Delta$, Δ is the step between the spectral points, $i = -(M-1)/2, \ldots (M-1)/2$, M is the number of points in digitized spectrum.

The aim of the current study is to estimate the refractive index of the media inside the Fabry–Perot cavity with known geometrical length. However, as can be seen from the expression (6), if refractive index dispersion takes place, the task is underdetermined and some additional information, related to the refractive index is needed. Such information can be obtained from a spectral function fringe visibility V, as for example, in [14]. In such a manner, the approach for obtaining the refractive index is divided into the following steps:

(1) Initial estimation of the mean refractive index value according to the fringe visibility of the interferometer spectral function. For that a reference stable EFPI must be installed and the reflectivity of one of its mirrors must change due to the change of refractive index of a media outside the interferometer. In the current study we have utilized a wafer-based EFPI, with cavity formed by a crystalline silicone plate.

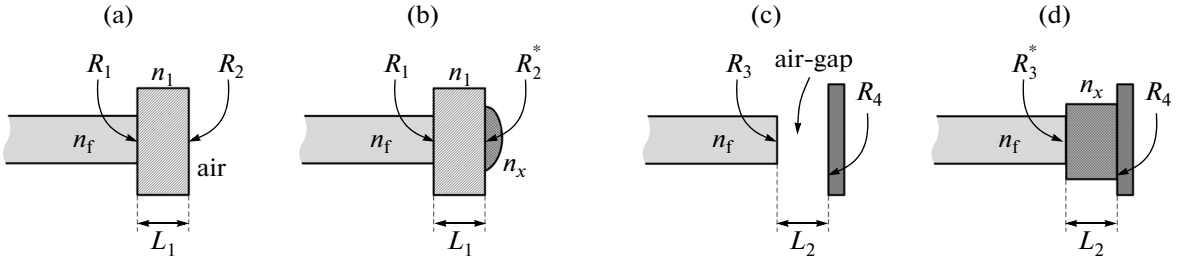

Fig. 1. Interferometers, used for finding the refractive index and the absorption of the investigated media.

The fiber was attached to the one face of the plate, on the other face a droplet of the material under study was put, changing the bound reflectivity:

$$R_2^*(\lambda) = \left(\frac{n_{\mathrm{Si}}(\lambda) - n_x(\lambda)}{n_{\mathrm{Si}}(\lambda) + n_x(\lambda)} \right)^2, \tag{8}$$

where $n_x(\lambda)$ is refractive index of the material under study.

For a known parameters of the interferometer a calibration curve $V(n_x)$ can be calculated, according to which the mean refractive index value is easily found.

(2) Estimation of the refractive index dispersion can be done with the use of another Fabry–Perot interferometer, in which cavity the analyzed material is placed. With the known mean refractive index value n_0, obtained at the first step, the calculated OPD of the interferometer with the material under study inside the cavity L_e and the real geometrical cavity length L_0, the expression for the refractive index dispersion can be easily obtained from the expression (6) and is written as follows:

$$\frac{dn}{d\lambda} = \left(n_0 - \frac{L_e}{L_0} \right) \Big/ \lambda_0 . \tag{9}$$

When calculating L_e it must be assumed that the interferometer is air-gap.

3. NANOPARTICLE-ARABINOGALACTAN COMPOSITE PREPARATION

Typically, synthesis of nanometer-sized particles is performed by either destruction of a solid material, or by various condensation methods: high temperature evaporation, concretion from a flux, chemical reduction of a metal salt. The latter allows one to control the shape and the size of the produced particles by selecting the proper conditions of the chemical reaction. In order to prevent the particles adhesion, a special component—a stabilizer is added to the reaction, separating the produced particles. An approach for nanoparticles synthesis by chemical reduction of a metal salt by an arabinogalactan solution is of a great interest. This complex organic material is primarily extracted from larch wood, in which it's concentration can reach about 10–15%. AG demonstrates a unique combination of properties: water solubility, permeability through cell barriers, immune-modulation, optical activity, as well as the production simplicity.

During the chemical reaction of arabinogalactan with metal salts, the chemical reduction takes place, as a result, metallic particles with dimensions about 5–20 nanometers [15], surrounded by AG molecules, are formed. In this case, arabinogalactan acts as a reducing agent and a stabilizer simultaneously, and limits the growth of the particles sizes. The resultant metal-organic nanocomposite inherits such arabinogalactan properties, as water solubility and cell barrier permeability, which provides it's applications in medicine, biology and optics.

4. EXPERIMENTAL SETUP

In order to implement the proposed approach, we needed to perform the measurement of four interferometers spectra: one with known OPD and optical losses inside the cavity, with one of the mirrors formed by Fresnel reflection from a bound of two known media (some solid and an air, for instance)—see Fig. 1a; the second, different from the first interferometer in that the second mirror is formed by the bound of the same solid and the droplet of material under study—see Fig. 1b; the third, an air-gap EFPI—see

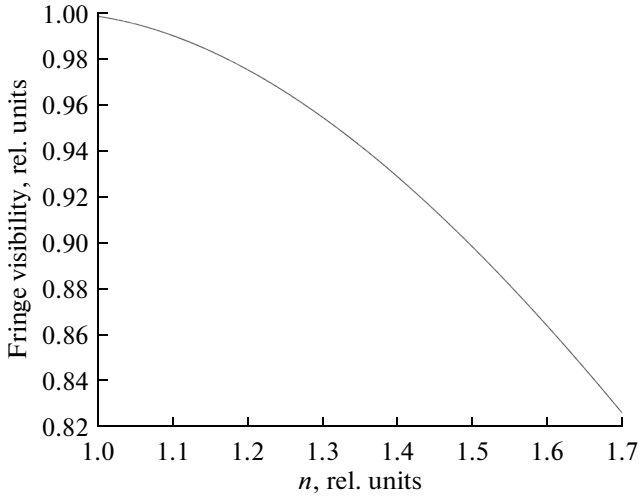

Fig. 2. Calibration curve of the interferometer spectrum fringe visibility and the refractive index of the media at the right side of the Si plate.

Fig. 1c; and the fourth one, different from the third in that the cavity was filled with the material under study—see Fig. 1d.

Interferometers spectra measurements were carried out with the help of the optical sensor interrogator National Instruments PXIe 4844, installed into PXI chassis PXIe 1065 and controlled by PXIe 8106 controller. The spectrometer parameters are the following: the scanning range is 1510–1590 nm (spectral interval width $\Lambda = 80$ nm), the spectral step $\Delta = 4$ pm (number of spectral points $M = 20001$), the scanning speed $k_\lambda = 2400$ nm/s, the spectrum acquisition time $T_M \approx 0.035$s and the output power $P \approx 0.06$ mW.

For the initial estimation of the refractive index (in the interferometers in Figs. 1a and 1b) we have used a plate of a crystalline silicon with width about 240 μm. A calibration curve relating the interferometer spectrum fringe visibility with the refractive index of the medium at the right side of the plate is shown in Fig. 2. The curve was calculated analytically with the use of the Gaussian beam formalism, applied to the Fabry–Perot cavity [9]. The cavity parameters were substituted the same as the practical ($L_0 = 240$ μm, silicon inside the cavity). Before measuring the spectrum of each droplet, the spectrum of fiber-plate-air configuration (Fig. 1a) was measured in order to take into account possible tilt between the plate and the fiber.

Spectral functions of the Si-plate interferometers with air, arabinogalactan and Mn-composite are shown in Fig. 3. From the measured spectra we have found the initial estimates of AG and Mn-nanoparticle-AG composite refractive indexes: $n_{0AG} \approx 1.488$ and $n_{0AG + Mn} \approx 1.516$. The refractive index of AG + Ni-nanoparticle composite was measured analogously and is $n_{0AG + Ni} \approx 1.503$.

After this first step, the refractive index dispersions were calculated. For that, an air-gap EFPI with fixed cavity length $L_0 = 1883$ μm was installed. The reflectivity of the second mirror was ~90%. At first, it's spectral function was measured, from which the exact cavity length value was calculated according to the approach [12]. After that, the cavity was filled by the material under study, and its spectral function was measured. Then the OPD L_e was calculated according to the approach [12], assuming that the cavity is air-gap. Therefore, the refractive index dispersion could be calculated according to the expression (9). The spectral functions of the interferometers with air, arabinogalactan and AG+Mn particle composite are shown in Fig. 4.

The calculated values of the refractive index dispersions $dn/d\lambda$ were ~0.051 μm^{-1} for pure arabinogalactan, ~0.064 μm^{-1} for AG + Mn nanoparticle composite and ~0.057 μm^{-1} for AG + Ni nanoparticle composite. The attenuations calculated from the above spectral functions are ~1.405 dB/mm for AG, ~3.03 dB/mm for AG + Mn nanoparticle composite and ~2.18 dB/mm for AG + Ni nanoparticle composite.

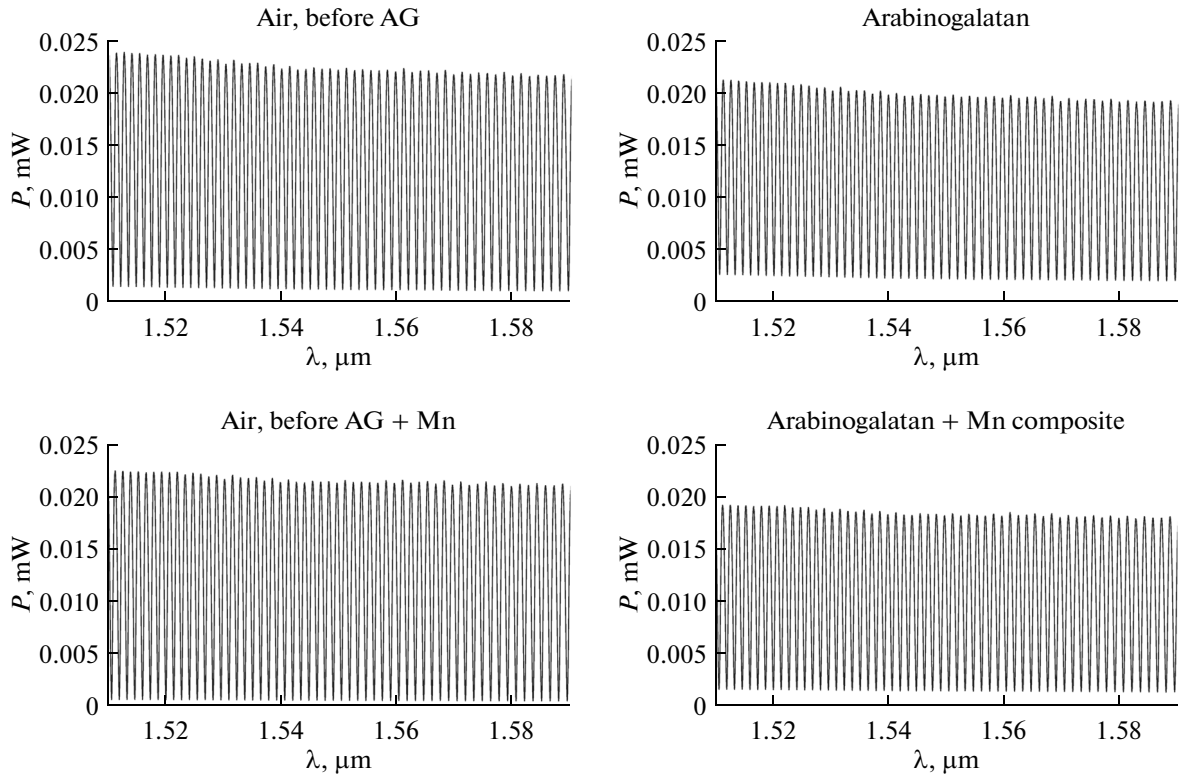

Fig. 3. Spectral functions of the reference Si-plate interferometer with air, AG and AG + Mn composite on the right side of the plate.

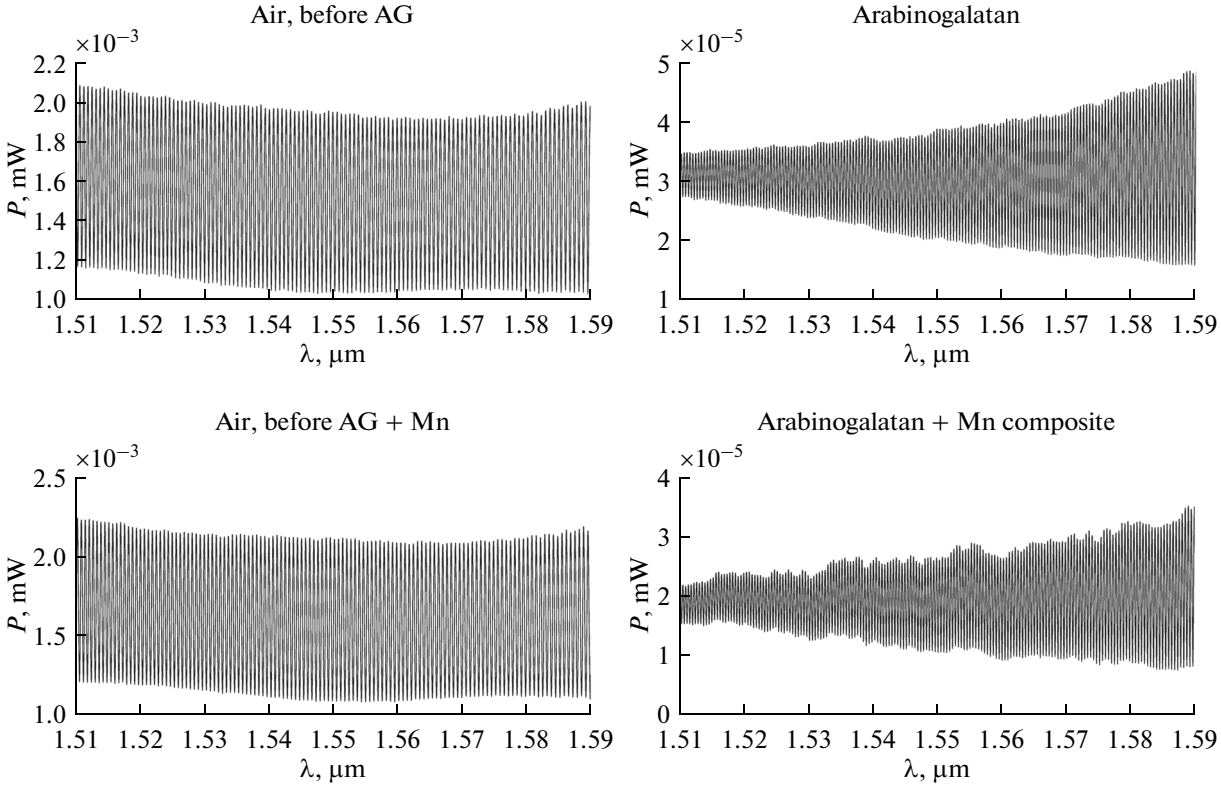

Fig. 4. Spectral functions of the interferometers with air, AG and Ag + Mn particle composite.

5. CONCLUSIONS

In the current paper an approach for refractive index and refractive index dispersion measurement, based on the wavelength-domain interferometry was presented. With the use of the proposed approach the influence of the metallic nanoparticle trapped by the arabinogalactan molecule on the refractive index and optical attenuation of the resultant AG+nanoparticle composite was investigated.

ACKNOWLEDGMENTS

The work was supported by the program State Tasks for Higher Educational Institutions (project nos. 3.1446.2014K and 2014/184).

REFERENCES

1. Kelly, K.L., Coronado, E., Zhao, L.L., and Schatz, G.C., The optical properties of metal nanoparticles: the influence of size, shape, and dielectric environment, *J. Phys. Chem., Ser. B*, 2003, vol. 107, pp. 668–677.

2. Castro, J.C.A., Surface plasmon resonance of a few particles linear arrays, *J. Electromagn. Anal. Appl.*, 2011, vol. 03, no. 11, pp. 458–464.

3. Jain, P.K., El-Sayed, I.H., and El-Sayed, M.A., Au nanoparticles target cancer, *Nanotoday*, 2007, vol. 2, no. 1, pp. 18–29.

4. Watson, C., Ge, J., Cohen, J., Pyrgiotakis, G., Engelward, B.P., and Demokritou, P., High-throughput screening platform for engineered nanoparticle-mediated genotoxicity using CometChip technology, *ACS Nano*, 2014, vol. 8, no. 3, pp. 2118–2133.

5. Schepetkin, I.A. and Quinn, M.T., Botanical polysaccharides: macrophage immunomodulation and therapeutic potential, *Int. Immunopharmacol.*, 2006, vol. 6, no. 3, pp. 317–333.

6. Polyakov, N. E., Magyar, A., and Kispert, L.D., Photochemical and optical properties of water-soluble xanthophyll antioxidants: aggregation vs. complexation, *J. Phys. Chem., Ser. B*, 2013, vol. 117, no. 35, pp. 10173–10182.

7. Wang, Z. and Jiang, Y., Wavenumber scanning-based Fourier transform white-light interferometry, *Appl. Opt.*, 2012, vol. 51, no. 22, pp. 5512–5516.

8. Saleh, B.E.A. and Teich, M.C., *Fundamentals of Photonics*, N.Y.: John Wiley & Sons, 1991, p. 947.

9. Ushakov, N.A. and Liokumovich, L.B., Resolution limits of extrinsic Fabry–Perot interferometric displacement sensors utilizing wavelength scanning interrogation, *Appl. Opt.*, 2014, vol. 53, no. 23, pp. 5092–5099.

10. Shen, F. and Wang, A., Frequency-estimation-based signal-processing algorithm for white-light optical fiber Fabry–Perot interferometers, *Appl. Opt.*, 2005, vol. 44, no. 25, pp. 5206–5214.

11. Ushakov, N.A. and Liokumovich, L.B., Investigation of baseline measurement resolution of a Si plate-based extrinsic Fabry–Perot interferometer, *Proc. SPIE*, 2014, vol. 9132, p. 913214.

12. Ushakov, N.A., Liokumovich, L.B., and Medvedev, A., EFPI signal processing method providing picometer-level resolution in cavity length measurement, *Proc. SPIE*, 2013, vol. 8789, p. 87890Y.

13. Han, M., Zhang, Y., Shen, F., Pickrell, G.R., and Wang, A., Signal-processing algorithm for white-light optical fiber extrinsic Fabry–Perot interferometric sensors, *Opt. Lett.*, 2004, vol. 29, no. 15, pp. 1736–1738.

14. Chen, J.-H., Zhao, J.-R., Huang, X.-G., and Huang, Z.-J., Extrinsic fiber-optic Fabry–Perot interferometer sensor for refractive index measurement of optical glass, *Appl. Opt.*, 2010, vol. 49, no. 29, pp. 5592–5596.

15. Sukhov, B.G., Aleksandrova, G.P., Grishchenko, L.A., Feoktistova, L.P., Sapozhnikov, A.N., Proidakova, O.A., T'kov, A.V., Medvedeva, S.A., and Trofimov, B.A., Nanobiocomposites of noble metals based on arabinogalactan: preparation and properties, *J. Struct. Chem.*, 2007, vol. 48, no. 5, pp. 979–984.